Crystal-plasticity finite-element analysis of deformation behavior in a commercially pure titanium sheet

Hama, T; Kobuki, A; Fujimoto, H; Takuda, H

Crystal-plasticity finite-element analysis of deformation behavior in a commercially pure titanium sheet

2016 J. Phys.: Conf. Ser. 734 032071

(http://iopscience.iop.org/1742-6596/734/3/032071)

Numisheet IOP Publishing
Journal of Physics: Conference Series **734** (2016) 032071 doi:10.1088/1742-6596/734/3/032071

Crystal-plasticity finite-element analysis of deformation behavior in a commercially pure titanium sheet

T Hama[1], A Kobuki[1], H Fujimoto[1], and H Takuda[1]

[1]Graduate School of Energy Science, Kyoto University, Yoshida-honmachi, Sakyo-ku, Kyoto 606-8501, Japan

E-mail: hama@energy.kyoto-u.ac.jp

Abstract. A crystal-plasticity finite-element method was used to examine the deformation mechanism in a commercially pure titanium sheet. The following tension-compression asymmetry was exhibited in the stress-strain curves: the yield stress was larger under tension than under compression, whereas the work-hardening was smaller under tension than under compression. The strain hardening behaviour was predicted qualitatively well using the crystal-plasticity analysis. The simulation results suggested that the tension-compression asymmetry could be explained in terms of the difference in the activity of the twinning systems.

1. Introduction

Commercially pure (CP) α-titanium (Ti) sheets are widely used in various products due to their characteristics such as high strength, corrosion resistance, and biological compatibility [1, 2]. CP-Ti sheets exhibit deformation behavior with strong anisotropy. One of the main factors of the anisotropy is that they have the hexagonal-close-packed (hcp) structure that depicts a strong crystalline anisotropy. Specifically, the critical resolved shear stress (CRSS) as well as work-hardening differs significantly depending on the family of slip systems [3]. The twinning systems, which have the direction dependence in deformation, also play a role as the secondary plastic deformation mode [4, 5]. Moreover, rolled CP-Ti sheets have the strong basal texture in which c-axes tilt 20 to 40° from the normal direction (ND) to the transverse direction (TD) [4-9]; thus, the anisotropy is further pronounced. However, the role of each slip or twinning system on the macroscopic anisotropic deformation behavior is not yet well understood.

A crystal-plasticity model enables a direct investigation into the interaction between mesoscopic crystalline and macroscopic deformation in metals. Therefore, a crystal-plasticity analysis is useful to investigate the deformation behavior in hcp metals that exhibit strong anisotropy, and it has widely been utilized for magnesium (Mg) alloys [10-15]. There are a few past studies that examine the deformation behavior in CP-Ti using a crystal-plasticity analysis [16, 17]. However, the simulation accuracy in the previous studies seems to be insufficient; thus, the deformation mechanism is still open to discussion.

In the present study, the tension-compression asymmetry observed in the stress-strain curves in a CP-Ti JIS Grade 1 sheet is investigated using a crystal-plasticity finite-element method. First, the stress-strain curves obtained under monotonic tension and compression are compared between simulation and experimental results to verify the simulation accuracy. The mechanism that yields the tension-compression asymmetry is then investigated numerically.

2. Crystal-plasticity model

The crystal-plasticity model employed in this study follows the model used in our previous studies for Mg alloy sheets [10, 11, 15]. The crystalline slip is assumed to follow Schmid's law. The slip rate $\dot{\gamma}^{(\alpha)}$ of the α slip system is assumed to be given by a visco-plastic power law as [18]

$$\frac{\dot{\gamma}^{(\alpha)}}{\dot{\gamma}_0} = \left| \frac{\tau^{(\alpha)}}{\tau_{\mathrm{Y}}^{(\alpha)}} \right|^{\frac{1}{m}} \mathrm{sign}\left(\tau^{(\alpha)}\right), \quad \dot{\tau}_{\mathrm{Y}}^{(\alpha)} = \sum_{\beta} q_{\alpha\beta} h \left| \dot{\gamma}^{(\beta)} \right| \tag{1}$$

where $\tau^{(\alpha)}$ and $\tau_{\mathrm{Y}}^{(\alpha)}$ are the Schmid's resolved shear stress and the current strength of the α slip system, respectively, $\dot{\gamma}_0$ is the reference strain rate, m is the rate sensitivity exponent, $q_{\alpha\beta}$ is the self ($\alpha = \beta$) and latent ($\alpha \neq \beta$) hardening moduli, and h is the hardening rate for which the following two laws are used.

$$h = h_0 \ \text{ and } \ h = h_0 \left(1 - \frac{\tau_0}{\tau_\infty}\right) \exp\left(-\frac{h_0 \bar{\gamma}}{\tau_\infty}\right) \ \text{ with } \ \bar{\gamma} = \sum_{\alpha} \int \left| \dot{\gamma}^{(\alpha)} \right| \mathrm{d}t. \tag{2}$$

In this study, five families of slip systems, i.e., basal {0001}<11$\bar{2}$0> slip, prismatic {10$\bar{1}$0}<11$\bar{2}$0> slip, pyramidal {10$\bar{1}$1}<11$\bar{2}$0> slip, pyramidal {11$\bar{2}$2}<11$\bar{2}$3> slip (hereafter termed as pyr <*a*+*c*>-1 slip), and pyramidal {10$\bar{1}$1}<11$\bar{2}$3> slip (hereafter termed as pyr <*a*+*c*>-2 slip), and two families of twinning systems, i.e., {10$\bar{1}$2} tensile twinning and {11$\bar{2}$2} compressive twinning, are taken into account. There are three basal, three prismatic, three pyramidal <*a*>, six pyr <*a*+*c*>-1, twelve pyr <*a*+*c*>-2, six {10$\bar{1}$2} twinning, and six {11$\bar{2}$2} twinning systems. The linear hardening (eq. (2)-1) is assumed for the twinning systems, and Voce hardening (eq.(2)-2) is assumed for the slip systems. A twinning and detwinning model proposed by the authors [10, 11, 15] is employed. The above rate-dependent crystal-plasticity model is incorporated into each Gauss point in a static finite-element method. The rate tangent modulus method [19] and the so-called generalized $r_{\min}$-strategy are employed for the explicit time integration [20].

3. Experimental and simulation procedures

In the experiment, a monotonic tension and compression test was conducted using a rolled CP-Ti JIS Grade 1 sheet with 1.0mm thick (Kobe steel) [5]. Comb-shaped dies were employed in the experiment to suppress the occurrence of buckling during compression.

A cube that had five uniform eight-node solid elements in each direction was used as a finite-element model. The same initial crystallographic orientation was assigned to all eight Gauss integration points in an element. The initial crystallographic orientations assigned to the elements were randomly selected from a result of EBSD measurement. The interaction matrix and hardening parameters employed in the present simulation are shown in Tables 1 and 2. Note that it was assumed that latent hardening due to twinning activity was larger than that of slip activity [7, 21]. Material parameters were carefully identified with referring to stress-strain curves and evolutions of Lankford value obtained under monotonic loading. Young's modulus, Poisson's ratio, and the rate-sensitivity exponent were respectively set to E = 105 GPa, ν= 0.34, and m = 0.02, which are the typical values for CP-Ti. The reference-strain rate was taken to be γ_0=0.001s^{-1}.

4. Results and discussion

Figure 1(a) shows the absolute stress-absolute strain curves obtained from the experiment and the simulation of monotonic tension and compression in the rolling direction (RD). In the experimental results, the yield stress is larger and the work-hardening is smaller under tension than under compression. Similar

Table 1. Latent-hardening parameters $q_{\alpha\beta}$ used in the present study.

	Basal	Prism	Pyr <a>	Pyr <a+c>-1	Pyr <a+c>-2	{10-12}	{11-22}
Basal	0.5	0.5	0.5	0.5	0.5	0.9	0.9
Prism	0.5	0.5	0.5	0.5	0.5	0.9	0.9
Pyr <a>	0.5	0.5	0.5	0.5	0.5	0.9	0.9
Pyr <a+c>-1	0.5	0.5	0.5	0.5	0.5	0.9	2.0
Pyr <a+c>-2	0.5	0.5	0.5	0.5	0.5	0.9	2.0
{10-12}	0.5	0.5	0.5	0.5	0.5	0.9	0.9
{11-22}	0.5	0.5	0.5	0.5	0.5	0.9	0.9

Table 2. Identified hardening parameters, in MPa.

	Basal	Prism	Pyr <a>	Pyr <a+c>-1	Pyr <a+c>-2	{10-12}	{11-22}
τ_0	133	62	81	145	145	90	140
τ_∞	180	160	210	270	270		
h_0	1950	1050	580	2050	2050	350	350

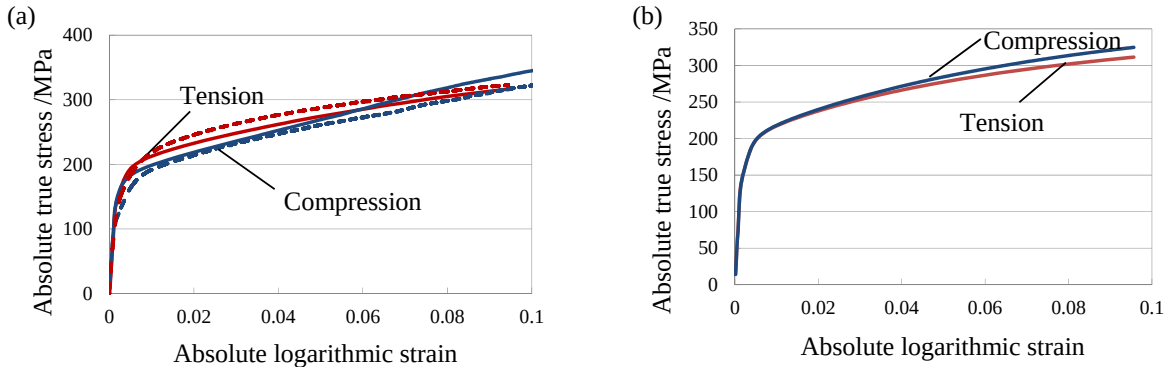

Figure 1. Stress-strain curves under tension and compression. (a) Results of experiment (dotted lines) and simulation (solid lines). (b) Simulation results obtained without considering twinning.

trends have been reported by Nixon et al. [7]. The strain hardening behavior is predicted qualitatively well in the simulation results.

The mechanism that yields the tension-compression asymmetry is examined using the evolution of relative activities (Figure 2). During tension, the activity of prismatic slip is dominant at the beginning of plastic deformation, and then the activities of pyramidal <a> slip and $\{11\bar{2}2\}$ twinning increase. These three systems are active until the end of deformation. The above activities of slip systems are similar under compression. In contrast, the twinning activity is different under compression as follows: the $\{10\bar{1}2\}$ twinning systems are active, and the $\{10\bar{1}2\}$ twinning activity under compression is larger than that of $\{11\bar{2}2\}$ twinning under tension. The differences in the twinning activities would play a significant role in the tension-compression asymmetry in the stress-strain curve because the CRSS of the $\{11\bar{2}2\}$ twinning is larger than that of the $\{10\bar{1}2\}$ twinning (Table 2) and the twinning activity is assumed to yield large latent hardening as described earlier (Table 1).

To confirm this discussion, Figure 1(b) shows the absolute stress-absolute strain curves under monotonic tension and compression in the RD obtained without considering twinning. Clearly, the yield stresses under tension and compression are almost identical and the difference in work-hardening is also reduced, exhibiting that the tension-compression anisotropy is largely owing to the differences in the twinning activities. On the other hand, the work-hardening is still slightly larger under compression than under tension. This difference may be due to the fact that the activity of pyramidal <a+c>-2 slip that has large CRSS and work-hardening rate increases gradually only under compression.

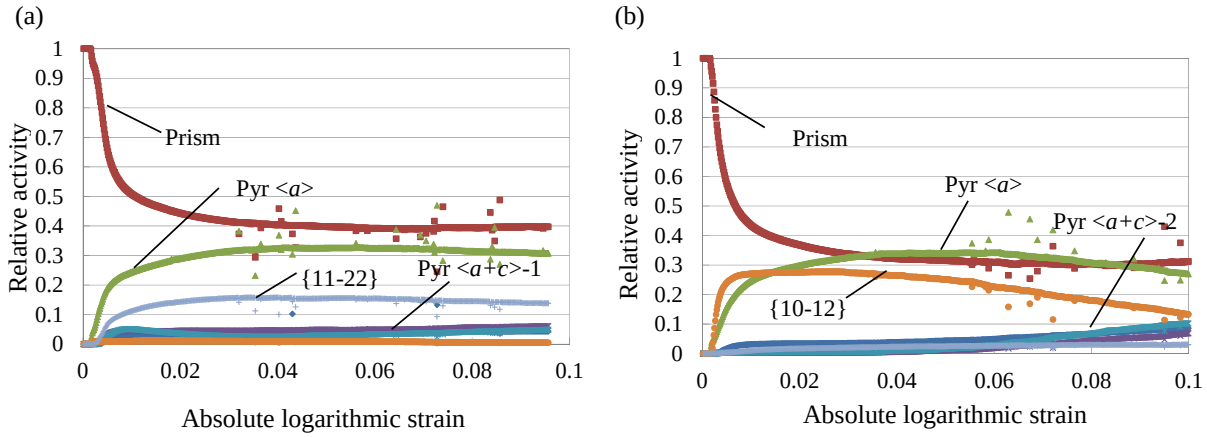

Figure 2. Relative activities obtained under monotonic (a) tension and (b) compression.

5. Conclusions

In the present study, the anisotropic deformation behavior under monotonic loading in the CP-Ti sheet was studied using the crystal-plasticity finite-element method. The tension-compression asymmetry exhibited in the stress-strain curves in the RD was predicted qualitatively well in the present simulation. The simulation results showed that the difference in the twinning activities was one of the main factors that yielded the tension-compression asymmetry.

References

[1] Ishiki M, Kuwabara T, Yamaguchi M, Maeda Y, Hayashida Y and Itsumi Y, *Trans. Jpn. Soc. Mech. Eng.* **75** (2009) 491-500.
[2] Zeng Z, Zhang Y, Jonsson S, *Mater. Des.* **30** (2009) 3105-3111.
[3] Yoshinaga H and Horiuchi R, *Trans. JIM* **5** (1963) 14-21.
[4] Hama T, Nagao H, Kobuki A, Fujimoto H, Takuda H, *Mater. Sci. Eng. A* **620** (2014) 390-398.
[5] Yi N, Hama T, Kobuki A, Fujimoto H, Takuda H, *Mater. Sci. Eng. A* **655** (2016) 70-85.
[6] Mullins S and Patchett BM, *Metall. Trans. A* **12** (1981) 853-863.
[7] Nixon ME, Cazacu O and Lebensohn RA, *Int. J. Plast.* **26** (2010) 516-532.
[8] Ishiyama S, *Titan. Japan* **54** (2006) 42-51 (in Japanese).
[9] Conrad H, Prog. *Mater. Sci.* **26** (1981) 123-403.
[10] Hama T and Takuda H, *Int. J. Plast.* **27** (2011) 1072–1092.
[11] Hama T and Takuda H, *Comput. Mater. Sci.* **51** (2012) 156-164.
[12] Graff S, Brocks W and Steglich D, *Int. J. Plast.* **23** (2007) 1957-1978.
[13] Hama T, Kitamura N and Takuda H, *Mater. Sci. Eng. A* **583** (2013), 232-241.
[14] Wang H, Wu PD, Wang J and Tome CN, *Int. J. Plast.* 49(2013), 36-52.
[15] Hama T, Tanaka Y, Uratani M and Takuda H, *Int. J. Plast.* (2016), in press.
[16] Gurao NP, Kapoor R, and Suwas S, *Acta Mater.*, 59(2011), 3431-3446.
[17] Benmhenni N, Bouvier S, Brenner R, Chauveau T, and Bacroix B, *Mater. Sci. Eng. A*, 573(2013), 222-233.
[18] Asaro RJ and Needleman A, *Acta Metall.* **33** (1985) 923-953.
[19] Pierce D, Asaro RJ and Needleman A, *Acta Metall.* **31** (1983) 1951-1976.
[20] Hama T, Nagata T, Teodosiu C, Makinouchi A and Takuda H, *Int. J. Mech. Sci.* **50** (2008) 175-192.
[21] Jain A and Agnew SR, *Mater. Sci. Eng. A* **462** (2007) 29-36.